Supporting Information

Maouche et al. 10.1073/pnas.1216939110

SI Materials and Methods

Reagents. Unless otherwise stated, all reagents were from Sigma-Aldrich: mouse anti-human CFTR (clone 24-1, 2 μg/mL) (R&D Systems), rabbit polyclonal antibodies anti-nAChR α7 (H-302, lot A2203, 1 μg/mL), anti–caveolin-1 (N-20, 10 μg/mL), anti-AC I (V-20, 2 μg/mL), and anti-AC III (C-20, 2 μg/mL) and goat polyclonal antibodies anti-AC VIII (R-20, 2 μg/mL) (Santa Cruz Biotechnology), Alexa Fluor 488 and Alexa Fluor 594 goat anti-mouse or anti-rabbit (IgG; 1:200) secondary antibodies (Molecular Probes), PHA 568487, SQ22536, thapsigargin, CGS 9343B, GF 109203X, KT 5720, and PD 98059 (Tocris Bioscience). The rabbit MPCT-1 anti-CFTR polyclonal antibody was kindly provided by R. L. Dormer (Department of Medical Biochemistry, University of Wales College of Medicine, Cardiff, United Kingdom) (1) and used to detect CFTR in murine respiratory tissue samples (2).

Human Airway Tissues. The use of human tissues was authorized by the bioethical law 94-654 of the Public Health Code of France, with a written consent from the patients or their families. Human airway tissues were collected after nasal polypectomy of patients who did not suffer from any other chronic airway disease. Human bronchial tissues from patients undergoing surgery for bronchial carcinoma were obtained from microscopically normal areas distant from the tumor.

Epithelial Cell Isolation and Culture. Human airway epithelial cells (HAECs) were isolated from polyps and bronchial tissues and cultured in an air–liquid interface condition as previously described (3). The cells were first induced to proliferate as a monolayer for about 10 d in a medium adapted from ref. 4 and consisting of Ham F-12/DMEM (1/3, vol/vol) supplemented with 0.87 μM bovine insulin, 65 nM human transferrin, 1.6 nM recombinant human epidermal growth factor, 1.38 μM hydrocortisone, 30 nM retinyl acetate, 9.7 nM 3,3′, 5-triiodo-L-thyronine, 2.7 μM (−)epinephrine, 35 μg/mL bovine pituitary extract, 5 μM ethanolamine, 5 μM o-phosphorylethanolamine, 30 nM sodium selenite, 1 nM manganese chloride tetrahydrate, 0.5 μM sodium metasilicate nonahydrate, 1 nM ammonium molybdate tetrahydrate, 5 nM ammonium vanadate, 1 nM nickel sulfate hexahydrate, 0.5 nM stannous chloride dihydrate, 100 units/mL penicillin, and 100 μg/mL streptomycin (HAEC proliferation medium). The cells were then cultured at an air–liquid interface for more than 20 d before use as previously described (3, 5). This results in cells organized as pseudostratified epithelium with differentiated ciliated cells expressing epithelial sodium channel and α7 nAChR at the apical membrane (3).

MM39, a cell line derived from the normal human airway glandular epithelium and expressing WT-CFTR (6), KM4, a cell line derived from cystic fibrosis (CF) human tracheal glands and homozygous for the ΔF508 mutation (7) were kindly provided by M. Merten (Faculté de Médecine, Université Henri Poincaré, Nancy, France), and were cultured in HAEC proliferation medium supplemented with 1% Ultroser G (BioSepra).

The vesicular stomatitis glycoprotein pseudotyped human lentiviral vector expressing the CFTR protein was produced, and HAECs or CF KM4 cells were transduced with the lentiviral vector expressing the CFTR cDNA as previously described (8, 9).

MM39 cells were cultured in 6- and 12-well plates (Beckton Dickinson) coated with type I collagen to study protein interaction by immunoprecipitation and $[cAMP]_i$, respectively, and in 4-well Lab-Tek II chambered coverglasses (Thermo Fisher) coated with type I collagen to study $[Ca^{2+}]_i$ and chloride secretion after α7 nAChR activation with PHA 568487 and chloride secretion after forskolin treatment.

Immunocyto/Histochemistry. An indirect immunofluorescence labeling technique was performed on frozen sections of bronchial tissues or cell cultures as previously described (10). All fluorescence-labeled preparations were examined with an AxioImager microscope or a LSM 710 confocal microscope (Zeiss) equipped with a Coolsnap FX camera (Roper Scientific). Images were processed with the AxioVision (Zeiss) and Photoshop (Adobe Systems) software.

Localization of Binding Sites for α-Bungarotoxin. α7 nAChR was also identified in human bronchial tissue samples by using fluorescent α-bungarotoxin (αBTX), as previously described (3).

Immunoprecipitation and Western Blotting. MM39 cells (2.10^7), cultured in six-well plates (Beckton Dickinson) coated with type I collagen, were lysed in RIPA buffer (10) to obtain whole cell protein extracts. To obtain membrane protein extracts, MM39 cells were successively washed with PBS, frozen, extensively washed with cold water, and proteins were extracted in 20 mM Tris·HCl pH 8, 137 mM NaCl, 10% (vol/vol) glycerol, 1% (vol/vol) Nonidet P-40, and 2 mM EDTA in the presence of protease inhibitors (Roche Diagnostics). Immunoprecipitations were carried out for 3 h at 4 °C, using 2 μg protein extract in the presence of 5 μg/mL anti-α7 nAChR antibody, 2 μg/mL anti-CFTR mAb, 2 μg/mL anti-AC1 antibody, 5 μg/mL anti-AC8 mAb, or isotype control antibody. Protein A/G sepharose beads were then added, and the samples were incubated for 4 h at 4 °C. Beads were washed five times with PBS, boiled in Laemmli sample buffer, and proteins were separated on 10% (wt/vol) SDS/PAGE gels under reducing conditions, transferred to nitrocellulose membranes, and blotted with antibodies using One-Step™ Complete IP-Western Kits (Genscript) according to standard manufacturer protocol. Signals were quantified with a Las-1000 camera (Raytest).

Transgenic Mice. All experiments and procedures were approved by the Ethics Committee for Animal Experimentation of the University of Reims Champagne-Ardenne, France. Mice, 10–12 wk of age, lacking the α7 subunit of the nAChR (C57BL/6J background) and wild-type littermates were generated as previously reported (11), shipped from Institut Pasteur (Paris), and housed in a sterile animal care facility. Similarly, mice lacking the α5, β2, or β4 nAChR subunit were generated as previously reported (12–14). CFTR$^{−/−}$ mice (C57BL/6J background) and wild-type littermates were generated as previously described (15) and maintained in the Institut de Transgénose (Unité Propre de Service 44 Centre National de la Recherche Scientifique, Orléans, France). CFTR$^{−/−}$ mice were made available by the French association Vaincre la Mucoviscidose.

Treatment of Mice with Nicotine. α7$^{+/+}$ or α7$^{−/−}$ mice received three i.p. injections of 1 mg/kg nicotine (nicotine tartrate salt) in normal saline (corresponding to one-third of the nicotine DL50 in mice: 3 mg/kg) 24 h, 16 h, and 1 h before measurements [nasal transepithelial potential difference (PD), mucociliary transport and ciliary beating frequency]. This treatment did not change mouse weight, food intake, and behavior both in control α7$^{+/+}$ mice and in α7$^{−/−}$ mice. Nicotine (α7$^{+/+}$ mice: 31 ± 22 nM, α7$^{−/−}$ mice: 35 ± 17 nM) and cotinine (α7$^{+/+}$ mice: 58 ± 42 nM, α7$^{−/−}$ mice: 68 ± 32 nM) blood concentrations were similar in nicotine-treated α7$^{+/+}$ and α7$^{−/−}$ mice after the 24-h nicotine treatment. These concentrations

are close to blood or plasma nicotine concentrations generally observed in cigarette smokers (62–230 nM) (16).

Transepithelial Potential Difference Measurements. Nasal transepithelial PD measurements were performed in mice using a Millicel-ERS epithelial tissue voltmeter (Millipore), as previously described (17). PD measurements were performed, at a flow rate of 80 µL/min, in the presence of normal saline, 0.1 mM amiloride, and 0.1 mM amiloride with 25 µM forskolin, successively. The thin capillary of the test electrode (Microloader; Eppendorf) was introduced ~5 mm into each nostril and the stable transepithelial PD was recorded during a minimal period of 15 s.

Studies of Halide Efflux. Studies of halide efflux were performed, using the halide-sensitive dye 6-methoxy-*N*-(3-sulfopropyl) quinolinium (SPQ), in HAECs cultured in air–liquid interface condition and in MM39, KM4, and KM4* (KM4 transfected with CFTR cDNA) cell lines cultured on glass-bottom dishes, as previously described (18). The chloride efflux was calculated by measuring the variation in SPQ fluorescence over a 2-min incubation period after the addition of forskolin.

Bioelectric Properties Measurements with Ussing Chambers. HAECs were cultured in air–liquid interface condition for 25–30 d. Thereafter, the Costar Transwell porous polyester membranes were detached and placed into an Ussing chamber and the bioelectric properties measured as previously described (18). Short-circuit current (Isc) was recorded in control condition or after a 3-h incubation with 0–10 µM αBTX. A total of 0.1 mM amiloride and 25 µM forskolin were added sequentially. Changes in Isc were calculated as the variations between the values measured immediately before the addition of reagents and the values corresponding to the plateau after the addition of reagents.

Measurement of Ionic Composition of Tracheal Surface Liquid. Native airway surface liquid was collected by a cryotechnique using a specially designed cryoprobe and ionic composition was analyzed by X-ray microanalysis as previously described (19, 20). This method permitted the simultaneous, nondestructive quantitative analysis of the biological elements of interest (Na, Cl, K, Ca, Mg, P, and S). The elemental concentration was calculated in millimoles per kilogram of dry weight.

Measurement of Mucus Transport Velocity in Mice. Mice were killed by i.p. injection of 550 mg/kg pentobarbital. The thorax was opened and from the trachea and a 5-mm length was cut and transferred to a delta T culture dish (Bioptechs) whose bottom was covered with a humidified filter paper. The trachea was opened longitudinally and 1 µL of a polystyrene fluorescent microspheres suspension (10 µm in diameter, fluospheres; Molecular Probes) was added on the epithelial surface at the lower part of the trachea. The dish was heated to 37 °C and placed on the stage of an upright microscope equipped with an epifluorescence setting (Axiophot; Carl Zeiss). The fluorescent microspheres were illuminated with a 450- to 490-nm bandpass filter and the emitted light was observed through a 520-nm highpass filter. Imaging was done with Axiovision software (Carl Zeiss) and the

AxiocamHS camera (Carl Zeiss) using a 5× objective. For each trachea, 60 images were recorded with an exposure time of 400 ms and a delay of 5 s between two images. To track individual microspheres, the plug-in "manual tracking" (http://rsb.info.nih.gov/ij/plugins/manual-tracking.html) in the ImageJ software (National Institutes of Health, Bethesda, MD) was used. From each image sequence, 5–10 microspheres were followed and their mean transport velocity was calculated. For each experimental condition, the trachea from 9 to 11 mice were used.

Measurement of Mucociliary Frequency of Murine Tracheal Epithelium. The mucociliary frequency was measured according to a technique previously described (21) and modified for the mouse (17). The principle of the method consisted of recording the frequency of the mucus waves propagated by the underlying cilia. After being anesthetized by i.p. injection of 10 mg/kg xylazine and 100 mg/kg ketamine, the mice were place in a supine position. The trachea was rapidly opened by a longitudinal incision and the mice were then introduced in a Plexiglas chamber at 37 °C with 100% relative humidity. The tracheal epithelium was illuminated by using a KL150B fiber optic source (Schott Mainz) and the reflected light allowed to visualize the variations in light intensity induced by the ciliary beating-dependent mucus waves. Specific epithelium areas where the mucociliary activity was visible were recorded through a NS50 stereomicroscope (Nachet) equipped with an objective of 8× magnification and a lateral extension tube to which a CCD camera was connected. The lateral ocular used had a 25× magnification. At least three different areas were recorded for 10 s at the rate of 50 images per second for each mouse trachea. The mucociliary activity was measured by analyzing the light-intensity variations using an image analysis technique developed through a plug-in of ImageJ (http://rsbweb.nih.gov/ij). From the video recordings, a region of interest was outlined by a graphical square with 50×50 pixel size and positioned over a ciliated cell area. From this region of interest, the gray level of each pixel was extracted over the 500 consecutive frames recorded. A fast Fourier transform (FFT) analysis was then used to analyze the brightness variations. From the FFT analysis, the spectrum distribution of the mucociliary frequency was displayed and for each spectrum the mean value of the frequency was calculated.

Measurement of $[cAMP]_i$ and $[Ca^{2+}]_i$. In the control and the PHA 568487 exposed MM39 cell line, intracellular cAMP content was measured, using cAMP enzyme immunoassays (Biotrak enzymeimmunoassay system; Amersham Pharmacia Biotech), according to standard manufacturer protocol.

The concentration of $[Ca^{2+}]_i$ was measured with the calcium-sensitive Fura-2 acetoxymethyl ester by a fluorescence ratiometric method as previously described (10).

Statistical Analyses. Except for curves illustrating the variations of $[Ca^{2+}]_i$, $[cAMP]_i$ and chloride secretion (SPQ fluorescence) where data were presented as mean ± SD, all data were expressed as median with maximal and minimal values and compared with the nonparametric Mann–Whitney test (*$P < 0.05$, **$P < 0.01$).
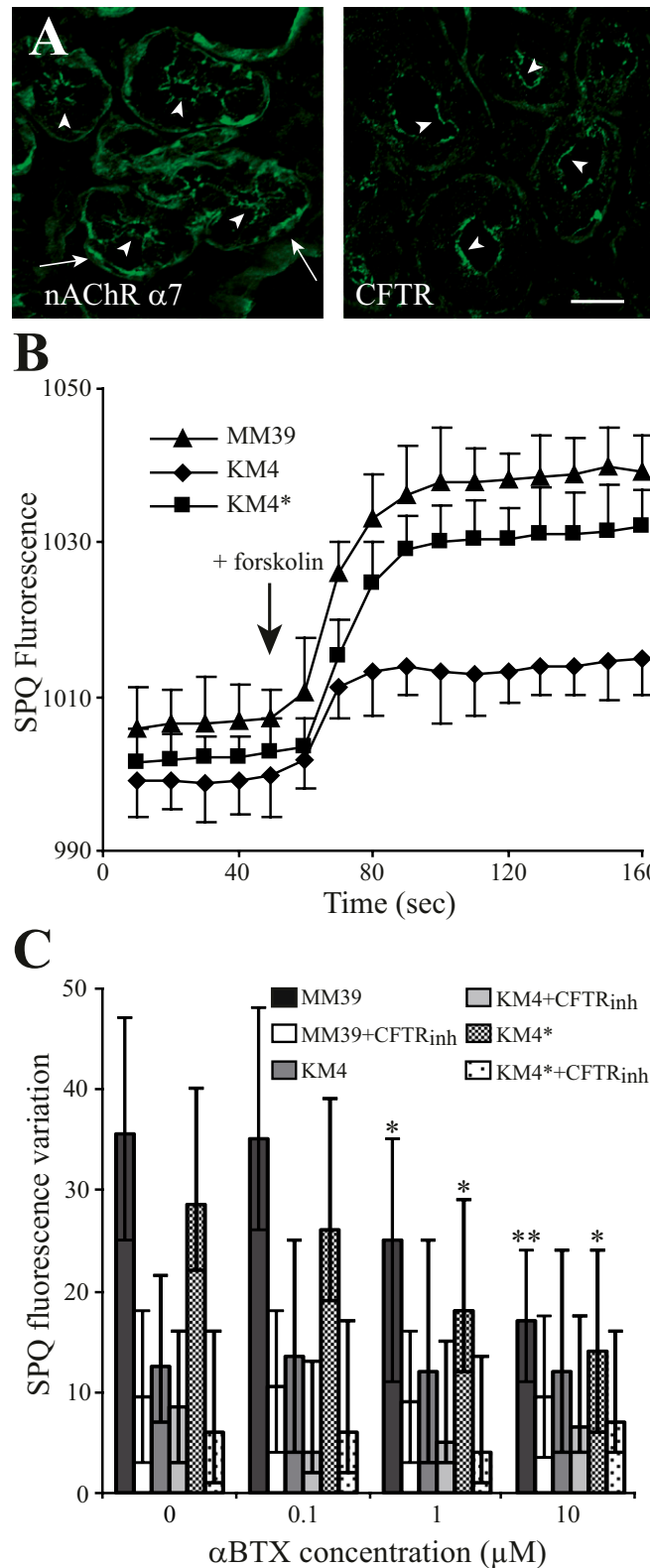
1. Mills CL, Pereira MM, Dormer RL, McPherson MA (1992) An antibody against a CFTR-derived synthetic peptide, incorporated into living submandibular cells, inhibits beta-adrenergic stimulation of mucin secretion. *Biochem Biophys Res Commun* 188(3): 1146–1152.
2. Doucet L, et al. (2003) Applicability of different antibodies for the immunohistochemical localization of CFTR in respiratory and intestinal tissues of human and murine origin. *J Histochem Cytochem* 51(9):1191–1199.
3. Maouche K, et al. (2009) alpha7 nicotinic acetylcholine receptor regulates airway epithelium differentiation by controlling basal cell proliferation. *Am J Pathol* 175(5): 1868–1882.
4. Lechner JF, LaVeck MA (1985) A serum-free method for culturing normal human bronchial epithelial cells at clonal density. *J Tissue Cult Methods* 9:43–48.

5. Hajj R, et al. (2007) Basal cells of the human adult airway surface epithelium retain transit-amplifying cell properties. *Stem Cells* 25(1):139–148.
6. Merten MD, et al. (1996) A transformed human tracheal gland cell line, MM-39, that retains serous secretory functions. *Am J Respir Cell Mol Biol* 15(4):520–528.
7. Kammouni W, et al. (1999) A cystic fibrosis tracheal gland cell line, CF-KM4. Correction by adenovirus-mediated CFTR gene transfer. *Am J Respir Cell Mol Biol* 20(4):684–691.
8. Castillon N, et al. (2004) Regeneration of a well-differentiated human airway surface epithelium by spheroid and lentivirus vector-transduced airway cells. *J Gene Med* 6(8): 846–856.
9. Baconnais S, et al. (2005) Abnormal ion content, hydration and granule expansion of the secretory granules from cystic fibrosis airway glandular cells. *Exp Cell Res* 309(2): 296–304.

10. Tournier JM, et al. (2006) alpha3alpha5beta2-Nicotinic acetylcholine receptor contributes to the wound repair of the respiratory epithelium by modulating intracellular calcium in migrating cells. *Am J Pathol* 168(1):55–68.

11. Orr-Urtreger A, et al. (1997) Mice deficient in the alpha7 neuronal nicotinic acetylcholine receptor lack alpha-bungarotoxin binding sites and hippocampal fast nicotinic currents. *J Neurosci* 17(23):9165–9171.

12. Picciotto MR, et al. (1995) Abnormal avoidance learning in mice lacking functional high-affinity nicotine receptor in the brain. *Nature* 374(6517):65–67.

13. Xu W, et al. (1999) Multiorgan autonomic dysfunction in mice lacking the beta2 and the beta4 subunits of neuronal nicotinic acetylcholine receptors. *J Neurosci* 19(21):9298–9305.

14. Salas R, et al. (2003) The nicotinic acetylcholine receptor subunit alpha 5 mediates short-term effects of nicotine in vivo. *Mol Pharmacol* 63(5):1059–1066.

15. Snouwaert JN, et al. (1992) An animal model for cystic fibrosis made by gene targeting. *Science* 257(5073):1083–1088.

16. Schneider NG, Olmstead RE, Franzon MA, Lunell E (2001) The nicotine inhaler: Clinical pharmacokinetics and comparison with other nicotine treatments. *Clin Pharmacokinet* 40(9):661–684.

17. Zahm JM, et al. (1997) Early alterations in airway mucociliary clearance and inflammation of the lamina propria in CF mice. *Am J Physiol* 272(3 Pt 1): C853–C859.

18. Delavoie F, et al. (2009) Salmeterol restores secretory functions in cystic fibrosis airway submucosal gland serous cells. *Am J Respir Cell Mol Biol* 40(4):388–397.

19. Baconnais S, et al. (1998) X-ray microanalysis of native airway surface liquid collected by cryotechnique. *J Microsc* 191:311–319.

20. Zahm JM, et al. (2001) X-ray microanalysis of airway surface liquid collected in cystic fibrosis mice. *Am J Physiol Lung Cell Mol Physiol* 281(2):L309–L313.

21. Puchelle E, Zahm JM, Sadoul P (1982) Mucociliary frequency of frog palate epithelium. *Am J Physiol* 242(1):C31–C35.
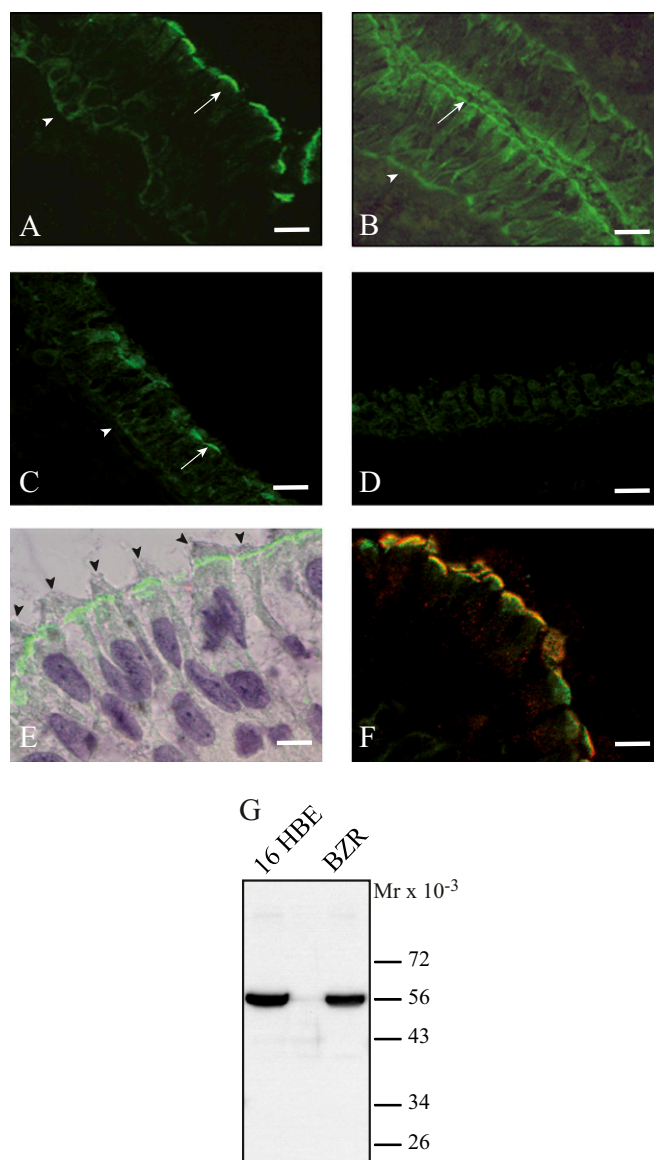
Fig. S1. Localization of α7 nAChR in the human and murine airway epithelium. α7 nAChR (green) is localized with the H-302 antibody (lot A2203) (*A* and *C–F*) or with Alexa Fluor 488-α-bungarotoxin (*B*) in human bronchial tissue samples, both at the apex of the airway epithelium (arrows) and in basal epithelial cells (arrowheads) (*A* and *B*). A similar localization is observed in the airway epithelium of wild-type mice (*C*), whereas only background staining is observed in α7$^{-/-}$ mice (*D*). (*E*) α7 nAChR is identified at the apical membrane of ciliated cells in human airway epithelium (arrowheads: cilia). (*F*) Localization of CFTR (red) and of α7 nAChR (green) by confocal microscopy at the apical membrane of ciliated cells in human airway epithelium. Yellow color illustrates the colocalization of α7 nAChR with CFTR. (*G*) By Western blot technique, the H-302 antibody recognizes one protein band at about 55 kDa, corresponding to the expected M_r of the α7 nAChR subunit, in protein extracts from 16HBE14o- and BZR cell lines, both derived from the normal human bronchial epithelium. [Scale bars: 15 μm (*A* and *B*), 20 μm (*C* and *D*), and 10 μm (*E* and *F*).]

Fig. S2. Airway mucus transport in $\alpha7^{-/-}$, $\alpha5^{-/-}$, $\beta2^{-/-}$, and $\beta4^{-/-}$ mice. Only mucus transport in $\alpha7^{-/-}$ mice is significantly different (71% decrease) from that observed in control C57BL/6J mice.

**Fig. S3.** α7 nAChR modulates chloride secretion in human airway glandular cells. (*A*) Localization of α7 nAChR and CFTR in glands from human bronchial tissue samples. α7 nAChR and CFTR are identified at the apical side of the glandular epithelium (arrowheads), α7 nAChR is also identified in myoepithelial cells at the periphery of glands (arrows). (Scale bar, 20 μm.) (*B* and *C*) SPQ flurorescence variations, induced by 25 μM forskolin in the presence of 0.1 mM amiloride, in three glandular cell lines: MM39, a cell line derived from the normal human airway glandular epithelium and expressing WT-CFTR, KM4, a cell line derived from CF human tracheal glands and homozygous for the ΔF508 mutation, and KM4*, a cell line derived from the KM4 cell line after transduction with the lentiviral vector expressing WT-CFTR cDNA (*B*) and effect of a preincubation with 10 μM CFTR$_{inh}$-172 for 1 h and αBTX (0–10 μM) for 3 h (*C*). Results are presented as mean ± SD for 12 different cells (*B*) or as median, with maximal and minimal values, for six different experiments and compared with the Mann–Whitney test

to the corresponding control in the absence of drug (*C*, *$P < 0.05$, **$P < 0.01$). CFTR residual activity in the KM4 cell line is about 45% of that measured in the MM39 cell line, a ratio increased to 88% in the KM4* cell line (*B*). αBTX exposure (1–10 μM) reduced CFTR activity only in MM39 and KM4* cell lines, an effect abolished in the presence of 10 μM CFTR$_{inh}$-172 (*C*).
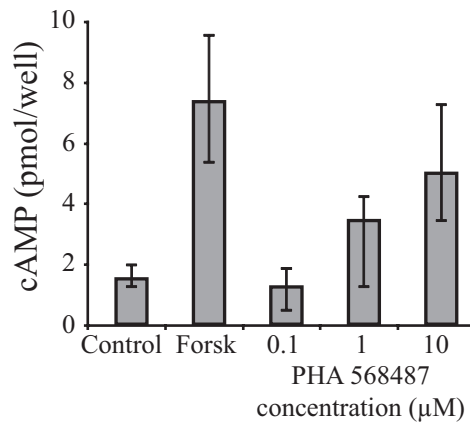
Fig. S4. PHA 568487 dose-dependent increase of intracellular cAMP. MM39 cells were exposed for 3 min to PHA 568487 (0–10 μM) and intracellular cAMP was measured. The result of direct activation of adenylate cyclases with 25 μM forskolin (Forsk) is also presented. Results are presented as median, with maximal and minimal values, and correspond to three independent experiments. The maximal PHA-induced [cAMP]$_i$ elevation was not significantly different from that observed in the presence of forskolin, suggesting that activation of α7 nAChR with PHA 568487 induced variations of [cAMP]$_i$ close to that observed after forskolin-induced direct activation of adenylate cyclases.
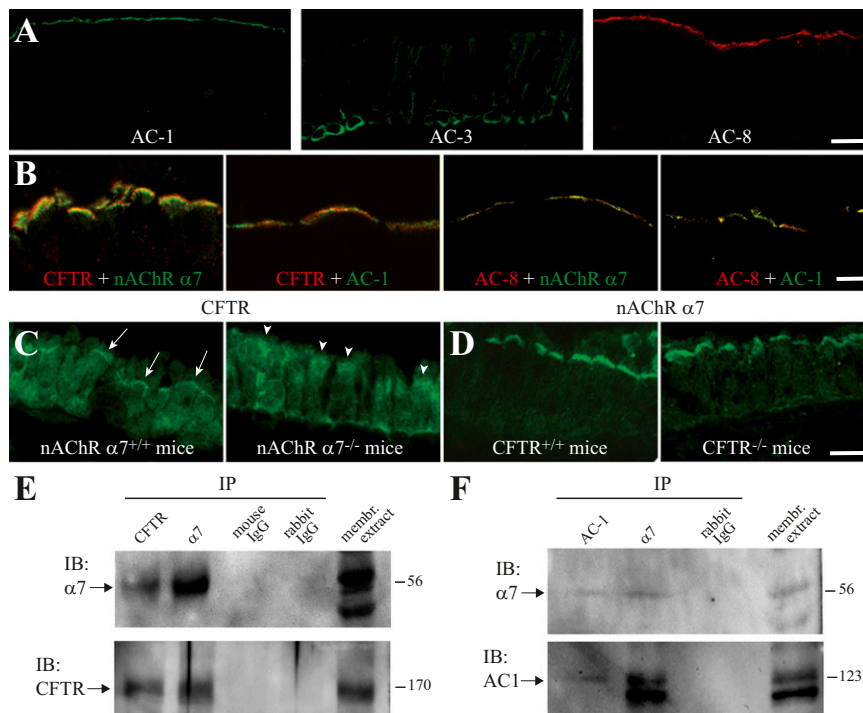
Fig. S5. α7 nAChR is associated with CFTR and AC-1 at the apical membrane of airway ciliated cells. (*A*) Localization of AC-1, -3, and -8 in the human airway epithelium. (*B*) Distribution (confocal microscopy) of CFTR and α7 nAChR, of CFTR and AC-1, of AC-8 and α7 nAChR and of AC-8 and AC-1 at the apical membrane of ciliated cells in human bronchial tissue samples. Molecules in red and green were detected with Alexa 594 and Alexa 488 conjugates, respectively. (*C* and *D*) Localization of CFTR in the airway epithelium of α7$^{+/+}$ nAChR and α7$^{-/-}$ nAChR mice (*C*) and of α7 nAChR in the airway epithelium of CFTR$^{+/+}$ and CFTR$^{-/-}$ mice (*D*). CFTR is present at the apical plasma membrane of tracheal epithelial cells in α7$^{+/+}$ nAChR mice (arrows) and intracellularly delocalized at the apex of epithelial cells in α7$^{-/-}$ nAChR mice (arrowheads) (*C*). (*E* and *F*) Immunoprecipitation and Western blot analysis of CFTR and α7 nAChR (*E*) and of AC-1 and α7 nAChR (*F*) in membrane protein extracts from MM39 cells in culture. Controls included rabbit and mouse control antibodies used in the i.p. procedure, and membrane protein extracts. Molecular weights ($M_r \times 10^{-3}$) of protein bands are reported on the *Right*. (Scale bars: 20 μm (*A*, *C*, and *D*) and 5 μm (*B*).
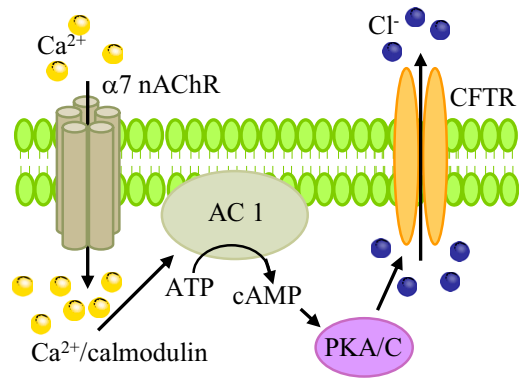
Fig. S6. Putative mode of CFTR regulation by the α7 nAChR.